Data assimilation with state alignment using high-level image structures detection

Alexandros Makris and Nicolas Papadakis
MOISE Team, Laboratoire Jean Kuntzmann (UMR 5224) / Inria Rhônes-Alpes
Campus de Saint Martin d'Hères, 38041 Grenoble, FRANCE
Email: firstname.lastname@imag.fr

***Abstract*—Sequential and variational assimilation methods allow tracking physical states using dynamic prior together with external observation of the studied system. However, when dense image satellite observations are available, such approaches realize a correction of the amplitude of the different state values but do not incorporate the spatial errors of structure positions. In the case of the position of a vortex, for example, when there is misfit between state and observation, the processes can be long to converge and even diverge when high dimensional state spaces are treated with few iterations of the assimilation methods as it is the case in operational algorithms. In this paper, we tackle this issue by proposing an alignment method based on modern object detection methods that uses visual correspondences between the physical state model and the structural information given by a sequence of image observing the phenomena.**

I. Introduction

Analysis and forecast of atmospheric and oceanic processes is of great scientific and practical interest. A large amount of satellite data that can be used towards that goal has been made available during the last decades. Efficient use of these data and particularity in parallel with an appropriate physics model is a challenging research topic. A main advantage of the satellite images comes from the spatial structure of the data. In particular, such spatial observations can be used to correct the error of positions of structures contained in the physics of interest. For example satellite imagery (e.g. SST, color) of the oceans can be used to characterize its dynamics since surface contour statistics extracted from these images are related to the underlying flow [13]. Therefore, automatic detection of geophysical structures is very important for many applications such as climate monitoring, forecasting, and ecosystem assessment.

A common situation in many assimilation problems where a grid state representation is used is that several coherent structures exist in both state and observation spaces but are not aligned. The proposed solution to this problem is to include displacement variables, this way displacement and amplitude errors can be handled simultaneously by the assimilation framework [21]. Here we propose to perform the alignment in a local object level by aligning the positions of the detected observation structures with the corresponding model structures. By working on the object level, we exploit the information rich areas of the image observations that are related with these structures and on the same time we discard noisy spurious features that commonly exist throughout the image. Before going into further details, let us briefly review the different existing methods in the domains of image assimilation and feature detection.

A. Image assimilation

In the literature, the assimilation of image data has been considered in different ways, that may be classified in three main categories: Pseudo observation, direct observation, and assimilation with state alignment.

Pseudo observation There are many works that try to estimate velocity fields from a series of image sequences through image processing optical flow methods [6], [25]. These kind of approaches have several limitations. Firstly, they require a series of images without missing data. Additionally, as they can only estimate the projection of the field on the gradient of the image intensity, the problem is ill-posed and a regularity prior is needed in order to close the problem and reconstruct the 2D velocity field.

Data assimilation techniques can be used to overcome the aforementioned limitations. These methods consider a hidden state to represent the field that has to be estimated, a dynamic model for the state, and a measurement model that links the state with the observation. Hence, the popular 4D-Var approach has been used in [12] for estimating the ocean surface velocity field. This technique uses Sea surface Temperature (SST) images and consider an Extended Image Model driven by a shallow water approximation for the dynamics of the velocity field. The output of this procedure (the estimated velocity field) has been used as pseudo-observation in an operational oceanic model.

Direct observation Modeling the error of pseudo-observations is a hard task, since they include data noise and image processing errors and the direct assimilation of images is preferable in practice [20], [24]. As a consequence, sequential and variational assimilation methods have been used for the direct estimation of the underlying dynamics given a sequence of images. Numerous works including Ensemble Kalman Filter [8] or 4D-var [20] have then been proposed to directly link the dynamics of the image sequence with the velocity of the physical model. Such approaches use the optical flow relations based on the conservation of the luminance along the image sequence. A main advantage is that the spatial consistency of the velocity field is here induced by the underlying dynamics and the regularity prior of optical flow techniques is no more needed.

These methods use a simple dynamic model to assimilate the data which might not be a good approximation to the observed system. In [24], another approach which directly assimilates the observation into the complete physical model is presented. The authors propose to increase the state dimension

with a passive tracer corresponding to the quantity observed in the image sequence. Instead of working at the pixel level, they extract and assimilate high level structures such as fronts or eddies (with curvelet transform). This technique allows to filter out the noise that exist on the raw data level and preserve the information rich areas. The link between physical quantities computed from the model (Lyapunov coefficients) and spatial gradients of chlorophyll satellite images have also been studied in [7] to solve the image assimilation problem.

Assimilation with state alignment All the prevous methods just assimilate the amplitude of the observed variables and do not allow dealing correctly with the misfits of structure positions. Hence, another class of approaches to assimilate structured image information is to consider a state space that includes displacement parameters. Using these parameters the background state structures can be displaced to match the detected image structures. The 'bogussing' technique used in operational forecast centers is such an approach [26]. In [9], a methodology to include pseudo-observations of the potential vorticity (PV) field in an operational system using 4D-Var is presented. The pseudo-observations are computed by experts and are used to correct the background field of the model. In [14], an analysis of different types of errors, including alignment and amplitude errors is performed. The authors prove that considering both types of errors and performing a two-step estimation approach renders the nature of the amplitude errors gaussian. In [10], a variational technique is used that includes displacement and amplitude errors. The technique is further improved in [18] where an approach in order to regularize the solution is also proposed. In [21], a two steps assimilation procedure is proposed. The first step performs a field alignment to align the model state with the observation. The second step is the amplitude adjustment where classical data assimilation is performed. To do so a displacement vector for each grid cell is added to the state and estimated to provide the required alignment. In [16], pseudo-observations are used to align detected dry intrusions structures in water vapor (WV) images with the (PV) field.

B. Atmospheric-Oceanic Features Detection

In order to realize a correction of structure positions, the detection of image features describing the coherent structures is a crucial step. The approaches to detect features and in particular oceanic features such as fronts or eddies can be grouped into the following categories: gradient based edge detection [3], statistical edge detection methods [5], wavelet analysis [23] [27], level-set [1],surface fitting [11]. Let us describe these different approaches with respect to their applicative context.

The detection of fronts, namely in chlorophyll images, can be done using edge detection after the application of a context aware median filter [3] or with a histogram based method [4]. Let us also mention the work of [23], where a multi-resolution wavelet decomposition is employed to filter the image, before detecting fine edges. To deal with occlusions, fronts in cloudy regions are detected in [17] using multiple images over a short period of time and superimposing the detection using several heuristics. A method based on Canny algorithm to detect fronts using edge detection has also been proposed in [19], where an interpolation technique is finally used to fill sparse data. In the specific case of SST images, a maximum likelihood approach has been proposed in [11] to detect fronts. Local curvature statistics along the level-lines of SST images can also be used as descriptors of the geometry of the front regions [1].

The detection of general oceanic features has also been investigated. In [27] a method to detect oceanic features using synthetic aperture radar (SAR) observations is proposed. Screening of grayscale histograms is performed for feature detection, wavelet analysis for feature extraction, and classification based on texture analysis. The specific detection of coastal upwelling and filaments has been studied in [15]. The method has two stages, an initial coarse segmentation followed by structure growing to detect all the details. Such approaches based on a high-level description of the image features seem promising for a assimilation of general structures.

C. Outline of the paper

In this work, we propose a two steps assimilation method with field alignment. The first step performs the spatial alignment which is achieved through additional displacement state parameters. The second step corrects the amplitude of the state variables. To link the detected structures with the model variables, we increase the state dimension with a passive tracer corresponding to the quantity observed in the images. For the amplitude correction, standard techniques such as the Ensemble Kalman Filter or variational assimilation can be used. In this work we demonstrate the potential of the approach using optimal interpolation for amplitude corrections.

The main novelty of the method is the detection and matching of high level structures between the observation image and the synthetic model image. This technique allows us to use the most informative image regions to calculate the field alignment parameters, thus guarantying the robustness of the method. An interpolation scheme follows to complete the displacement field. To align the structures, we use the SURF [2] gradient based local descriptor which is a new approach to this end. Although, the global appearance of the structures that have to be detected varies significantly, it follows some general norms (e.g. eddies are expected to have a spiral-like form). This property renders the use of gradient based descriptors a suitable approach. The descriptor divides the region of interest into subregions and computes local histograms of gradients in each of these subregions. This way geometric information is preserved but on the same time the use of histograms in each subregion adds a considerable amount of flexibility by allowing local appearance variations.

The paper is organized as follows. In section II, we first recall the data assimilation problem. Then, we propose a theoretical alignment method in section III, describe the feature extraction and matching in section IV and finally demonstrate the potential of the approach in the experimental section V.

II. Data Assimilation Background

A. Model Definition

Let by $\mathbf{x}$ denote the n-dimensional state vector and by $\mathbf{z}$ the p-dimensional observation vector. The analysis and forecast state at time k are denoted by $\mathbf{x}_k$ and $\mathbf{x}_k^-$. The evolution of the model state is expressed in the discrete case as:

$$\mathbf{x}_k^- = M(\mathbf{x}_{k-1}) + \mathbf{e}_m \tag{1}$$

where $\mathbf{e}_m$ is the model error and M is a (non) linear operator describing the temporal evolution of the state variable. The model state is linked to the observations through the observation operator H. The observation operator links the state space $\mathcal{X}$ of dimension n to the observation space $\mathcal{Z}$of dimesion p:

$$\mathbf{z}_k = H(\mathbf{x}_k) + \mathbf{e}_o, \tag{2}$$

where $\mathbf{e}_o$ is the observation noise characterized by the covariance matrix $R = E[\mathbf{e}_o \mathbf{e}_o^T]$.

B. Probabilistic Formulation

From the bayesian perspective, the probability of the state $\mathbf{x}_k$ at time k given the measurements from time 0 to $k+n$ is:

$$p(\mathbf{x}_k|\mathbf{z}_{0:k+n}) \propto p(\mathbf{z}_{k:k+n}|\mathbf{x}_k) p(\mathbf{x}_k|\mathbf{z}_{0:k-1}) \tag{3}$$

where we assume that for every k the observation $\mathbf{z}_k$ given $\mathbf{x}_k$ is independent from the rest of the states and observations: $\mathbf{z}_k \perp \mathbf{z}_{1:k-1}, \mathbf{x}_{1:k-1}|\mathbf{x}_k$. Under the assumption of markovian dynamics i.e. $\mathbf{x}_k \perp \mathbf{x}_{0:k-2}|\mathbf{x}_{k-1}$ we get:

$$p(\mathbf{x}_k|\mathbf{z}_{0:k-1}) = \int p(\mathbf{x}_k|\mathbf{x}_{k-1}) p(\mathbf{x}_{k-1}|\mathbf{z}_{0:k-1}) d\mathbf{x}_{k-1} \tag{4}$$

The state evolution distribution $p(\mathbf{x}_k|\mathbf{z}_{0:k-1})$ is also referred to as background distribution and denoted as $p(\mathbf{x}_{b,k})$.

C. BLUE Estimator

In this section the least squares estimation (Best linear unbiased estimator) is presented. If the state evolution and measurement distributions of Section II-A are gaussian then the BLUE estimator is equal to the mean of the posterior of (3). The estimator performs a linearization of operator H: $H(\mathbf{x}) - H(\mathbf{x}_b) = \mathbf{H}(\mathbf{x} - \mathbf{x}_b)$ where $\mathbf{H}$ is the tangent linear operator of H. The BLUE estimate is given by:

$$\begin{aligned} \mathbf{x}_k &= \mathbf{x}_k^- + \mathbf{K}(\mathbf{z}_k - H(\mathbf{x}_k^-)) \\ \mathbf{K} &= B\mathbf{H}^T(\mathbf{H}B\mathbf{H}^T + R)^{-1} \end{aligned} \tag{5}$$

where B is the covariance matrix of the model error $\mathbf{e}_m$.

III. Assimilation using Object Alignment

The state vector $\mathbf{x}$ is defined over a regular grid. Let $\mathbf{x}_{[a]}$ denote the state of each grid cell and $\mathbf{x}_{[q]}$ define a translation for each cell. We denote by $\mathbf{z}_{[q]}$ the set of features that are used for the calculation of the displacement and by $\mathbf{z}_{[a]}$ the set of features that are used for the calculation of the amplitudes. The measurement vector now is: $\mathbf{z} = [\mathbf{z}_{[q]}, \mathbf{z}_{[a]}]^T$.

The goal is to jointly estimate the state and the displacement given the available measurements. By including the displacement vector in (3) we get:

$$p(\mathbf{x}_{[a]k}, \mathbf{x}_{[q]k}|\mathbf{z}_{0:k+n}) \propto p(\mathbf{z}_{k:k+n}|\mathbf{x}_{[a]k}, \mathbf{x}_{[q]k}) p(\mathbf{x}_{[a]k}, \mathbf{x}_{[q]k}|\mathbf{z}_{0:k-1})$$

The observation model $p(\mathbf{z}_{k:k+n}|\mathbf{x}_{[a]k}, \mathbf{x}_{[q]k})$ implies the translation of the initial field $\mathbf{x}_{[a]k}$ by $\mathbf{x}_{[q]k}$ and then the standard calculation of the amplitude discrepancy between the translated state and the observations. The observation model can now be decomposed as:

$$\begin{aligned} p(\mathbf{z}_{k:k+n}|\mathbf{x}_{[a]k}, \mathbf{x}_{[q]k}) =& p(\mathbf{z}_{[a]k:k+n}|\mathbf{x}_{[a]k}, \mathbf{x}_{[q]k}) \cdot \\ & p(\mathbf{z}_{[q]k:k+n}|\mathbf{x}_{[a]k}, \mathbf{x}_{[q]k}) \end{aligned} \tag{6}$$

If we consider that the appearance of the detected structures does not change rapidly we can make the following approximation:

$$p(\mathbf{z}_{[q]k:k+n}|\mathbf{x}_{[a]k}, \mathbf{x}_{[q]k}) \approx p(\mathbf{z}_{[q]k:k+n}|\mathbf{x}_{[a]k-1}, \mathbf{x}_{[q]k}) \tag{7}$$

With this approximation we can decouple the calculation of the $\mathbf{x}_{[a]}$ and $\mathbf{x}_{[q]}$ as:

$$\begin{aligned} p(\mathbf{x}_{[a]k}, \mathbf{x}_{[q]k}|\mathbf{z}_{0:k+n}) \propto & p(\mathbf{z}_{[a]k:k+n}|\mathbf{x}_{[a]k}, \mathbf{x}_{[q]k}) p(\mathbf{x}_{[a]k}|\mathbf{x}_{[q]k}, \mathbf{z}_{0:k-1}) \cdot \\ & p(\mathbf{z}_{[q]k:k+n}|\mathbf{x}_{[a]k-1}, \mathbf{x}_{[q]k}) p(\mathbf{x}_{[q]k}|\mathbf{z}_{0:k-1}) \end{aligned} \tag{8}$$

where: $p(\mathbf{x}_{[a]k}|\mathbf{x}_{[q]k}, \mathbf{z}_{0:k-1})$ is the amplitude prior and $p(\mathbf{x}_{[q]k}|\mathbf{z}_{0:k-1})$ is the displacement prior. The last two terms of (8) are used to calculate $\mathbf{x}_q$ which is performed approximately using a parametric structure description of lower dimension. An interpolation scheme is then used to calculate the complete displacement field, using as input the calculated structures displacements as described in Sec. IV. The updated $\mathbf{x}_q$ is then used to calculate $\mathbf{x}_a$. For the alignment step which is performed at a low dimension space a suitable method such as particle filtering can be used. For the amplitude update step, which is in a much higher dimension a variational scheme is more appropriate. The distribution $p(\mathbf{x}_{[a]k}|\mathbf{x}_{[q]k}, \mathbf{z}_{0:k-1})$ is the new background distribution for the amplitudes.

IV. Object Alignment Method

The object alignment requires the detection and matching of structures between the observation image and the synthetic model image contained in (or extracted from) the state variable $\mathbf{x}$. Gradient information is appropriate for the detection and the description of the structures since high gradients are commonly related to interesting geophysical formations. The structures are detected in the observation image and then a search for a match takes place in the synthetic image. Finally to calculate the alignment field an interpolation scheme is employed.

The proposed approach for structure detection has the following steps: (i) Computation of the gradient image, (ii) binarization of the gradient image using thresholding in order to locate high gradient regions, (iii) blob extraction from the binary image using size and convexity constraints appropriate for the application, (iv) calculation of the bounding box for each extracted blob.

The output of the detection is the list of the N detected image structures. Let by $\mathbf{s}_o^i$ denote the state of the i-th detected structure. In this work we consider rectangular shapes so their state is a 3-dimensional vector containing the x,y-image position and the size.

The next step is to find an appropriate descriptor in order to characterize the detected structures and match them with the synthetic image. Here we use the SURF [2] descriptor which relies on the distribution of the first order Haar wavelet responses in x and y direction. The descriptor of an image structure $\mathbf{s}_o^i$ is an 64-d feature vector $\mathbf{f}_o^i$.

For each detected image structure we look for an appropriate match in the synthetic model image with state vector $\mathbf{s}_m$ and descriptor $\mathbf{f}_m$. The search for each observation structure is performed using a sliding window approach on a dense grid of the synthetic image. Let each possible grid position be denoted by b and $\mathbf{s}_m^{(b)}$ be the corresponding structure. The match is given by:

$$b_{match} = \arg\min_b \|\mathbf{f}_m^{(b)} - \mathbf{f}_o^i\|_2 \tag{9}$$

The match is accepted if the norm between the descriptors is below a predefined threshold value. The displacement for the structure i, is given by: $\mathbf{x}_{[q]}^i = \mathbf{s}_o^i - \mathbf{s}_m^{(b_{match})}$

The set of computed displacement calculated from the matched structures is used to calculate the displacement field using irregular data interpolation [22]. The formula for computing the displacement value at a given position p is:

$$\mathbf{x}_{[q]}(p) = \frac{\sum_{i=1}^N w_i(p)\mathbf{x}_{[q]}^i}{\sum_{j=1}^N w_j(p)} \tag{10}$$

where the weight $w_i(p)$ of a structure i for a position p is inversely proportional to the distance between the position and the structure.

V. Experiments

To experimentally evaluate our approach we performed two series of experiments. In the first one we evaluate the structure detector/matcher using noisy observation from our experimental platform images and the corresponding numerical model output. In the second series we use simulated data which we assimilate with and without alignment. First of all, let us define the model and observation considered in our experiments.

A. Experimental framework

The experimental framework we considered to test the assimilation method is based on a Shallow-Water model [1] describing the evolution of a flow with a small depth. With respect to lake or river modeling, this representation includes the $2D$ surface velocity vector field (u, v) and the water height h. The dynamics of such variables is then given by the set of following hyperbolic partial differential equations:

$$\begin{cases} \partial_t h + \partial_x(hu) + \partial_y(hv) & = 0 \\ \partial_t(hu) + \partial_x(hu^2) + \partial_y(huv) + \frac{g}{2}\partial_x(h^2) & = 0 \\ \partial_t(hv) + \partial_x(huv) + \partial_y(hv^2) + \frac{g}{2}\partial_y(h^2) & = 0 \end{cases} \tag{11}$$

We then enriched the state with an additional tracer T. In real applications, such tracer can be a passive pollutant at the surface of the water. It can also represent the concentration of a product injected to a fluid in fluid mechanics experiments. The tracer can therefore be observed by external imaging processes (satellite or cameras). As the tracer is passive, its dynamics is driven by the surface velocity of our 2D model. By assuming that the mass of the tracer is preserved along time, its temporal evolution is given by the following PDE:

$$\partial_t T + \partial_x(Tu) + \partial_y(Tv) = 0. \tag{12}$$

With respect to previous notations, the model state is defined as: $\mathbf{x}_k = [h_k, u_k, v_k, T_k]$ and the dynamic operator M defined in relation (1) is given by equations (11) and (12).

Simulations of this model give us observations $\mathbf{z}_k = T_k$, that can be assimilated with the corresponding linear observation operator $H = [0, 0, 0, 1]$.

Remark Satellite images of the ocean such as Sea Surface Height (SSH) could be used in real applications. In this case, the passive tracer model is useless as we can directly observe h. However, as the shallow-water model is a rough approximation of the ocean dynamic, we rather not consider SSH data. In this paper, we prefer focusing on tracer observation to demonstrate the potential of our approach in a configuration that is coherent in terms of numerical model (2D shallow-water) and data (images of a tracer in a thin layer of water).

B. Structure Detection and Matching

To show the robustness of the detector we used the observation of our experimental platform and a corresponding shallow-water model synthetic image. The CORIOLIS (Grenoble, France) platform, simulates the evolution of a vortex in the atmosphere using a turntable which re-creates the effect of the Coriolis force on a thin layer of water. A complete rotation of the tank takes 60 seconds which corresponds to one Earth rotation. The vortex is created by stirring the water and made visible thanks to the addition of a passive tracer T. Photographs of the vortex are taken from above the turntable which constitute the observed image sequence. In this configuration, the evolution of the fluid can be represented with the shallow-water equations involving the surface velocity(u, v), where u and v are the zonal and meridional components of the velocity, and the water elevation h. Fig. 1 shows the detection and the matched structure using the methodology of Sec. IV. We observe that even though the images are noisy and the structures are not identical they are properly detected and matched. The two threshold values that concern the gradient magnitude image binarization and the acceptance of a possible match were manually set. These values are application specific and can be learn from a set of images with annotated structures.

C. Assimilation Experiments

As the experiment realized with the platform contain a single vortex, the situation is too simple for an interesting analysis. We therefore considered a synthetic example with two vortex (see Fig. 2) and applied the optimal interpolation method to estimate the dynamics of the system (u, v, h). We chose to initialize the system with a spatial shift of the variables (u, v, h, T) that would correspond in practice to a misfit of structure position (see first columns of Fig. 3

[1] http://verdandi.gforge.inria.fr

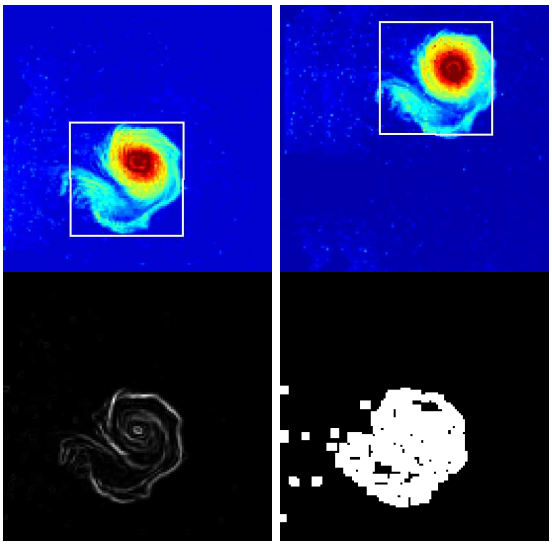

Fig. 1. Structures detection. Top left: Observation image z with the detected structure. Top right: Passive tracer T of the model with the matched structure. Bottom left: Gradient magnitude of the observation image. Bottom right: Thresholded gradient.

and 4). When assimilating observations of the passive tracer without state alignment, the process is long to converge. It also creates new structures by taking the mean of state tracer and observed tracer, as illustrated on the middle row of Fig. 3 and 4. On the other hand, one can observe on the last rows of these figures that the use of structure detection and of state alignment procedure allow a very accurate correction of the state variables, even after the assimilation of the first observation. From a qualitative point of view the structure information is perfectly recovered with the state alignment approach. On this synthetic experiment, the ground truth is known and a quantitative analysis can also be realized. To that end, we computed the Root Mean Square Error (RMSE) of the physic variables u, v and h estimated with and without state alignment. Fig. 5 then illustrates that the state alignment procedure allows a faster decrease of the RMSE.

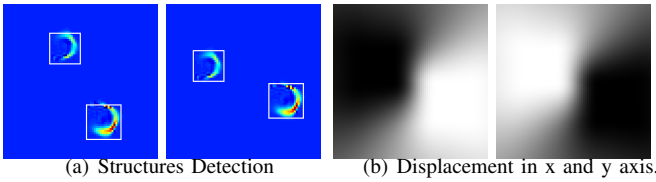

(a) Structures Detection (b) Displacement in x and y axis.

Fig. 2. (a) Detected structures on the measurement image and matched structures on the model image. (b) The resulting x-y displacement field. White color represents positive displacement values and black negative ones.

VI. Conclusion and perspectives

In this paper, we studied the use of computer vision tools in order to perform the alignment of physical state for assimilation purposes. The first results obtained on experimental data are very promising and show the feasibility of the use of structure of interest in satellite images to monitor numerical models. By extracting and matching features from observed images and model outputs, we propose a high level interpretation of the image content which remains robust to noise.

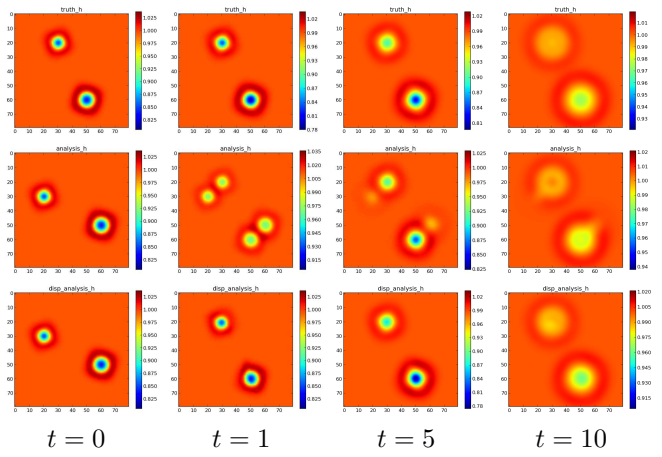

Fig. 3. State evolution of the water height h of the shallow water model on 80x80 domain. Top row: measurements. Middle row: optimal interpolation assimilation. Bottom row: optimal interpolation with state alignment. The tracer structures are initialized at bad locations (first column). When no state alignment is performed, the process realizes an interpolation between model structure and observed structures (middle row). The initial misfit of the structure position is corrected in one time step thanks to the state alignment process, which allows a faster convergence of the estimation (Fig. 5).

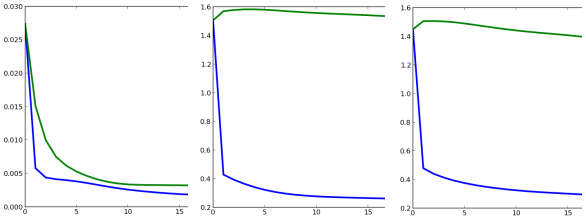

Fig. 5. RMS error evolution over 15 time steps for the height $h$and the u-v components of the velocity. The blue and green curve represents the evolution of the error with and without state alignment respectively. We note the sharp decrease of the error in the case with alignment on the first time step, where the alignment takes place. The method directly assimilates height values therefore the decrease of height error is sharp. The velocity is corrected indirectly, through the height, therefore its convergence rate is slower.

As a perspective, the learning of the image characteristics of the different physical structures that exist in reality in ocean satellite images (front, vortex...) will be a first task to identify and match better model to data.

In order to go towards operational problem, the next step will be to test the approach on real scenario. From the assimilation point of view, using strategies like Ensemble Kalman Filter instead of Optimal interpolation will also be the natural extension to this work.

Acknowledgment

The authors would like to acknowledge support from the ”pole MSTIC” of the Joseph Fourier University, the CNRS LEFE/MANU program and the SWOT/Ocean program from CNES.

References

[1] S. Ba, R. Fablet, D. Pastor, and B. Chapron, “Descriptors for sea surface temperature front regularity characterization,” in *IEEE Int. Geoscience and Remote Sensing Symposium (IGARSS’10)*, 2010, pp. 669 –672.

[2] H. Bay, A. Ess, T. Tuytelaars, and L. J. V. Gool, “Speeded-up robust features (surf),” *Computer Vision and Image Understanding*, vol. 110, no. 3, pp. 346–359, 2008.

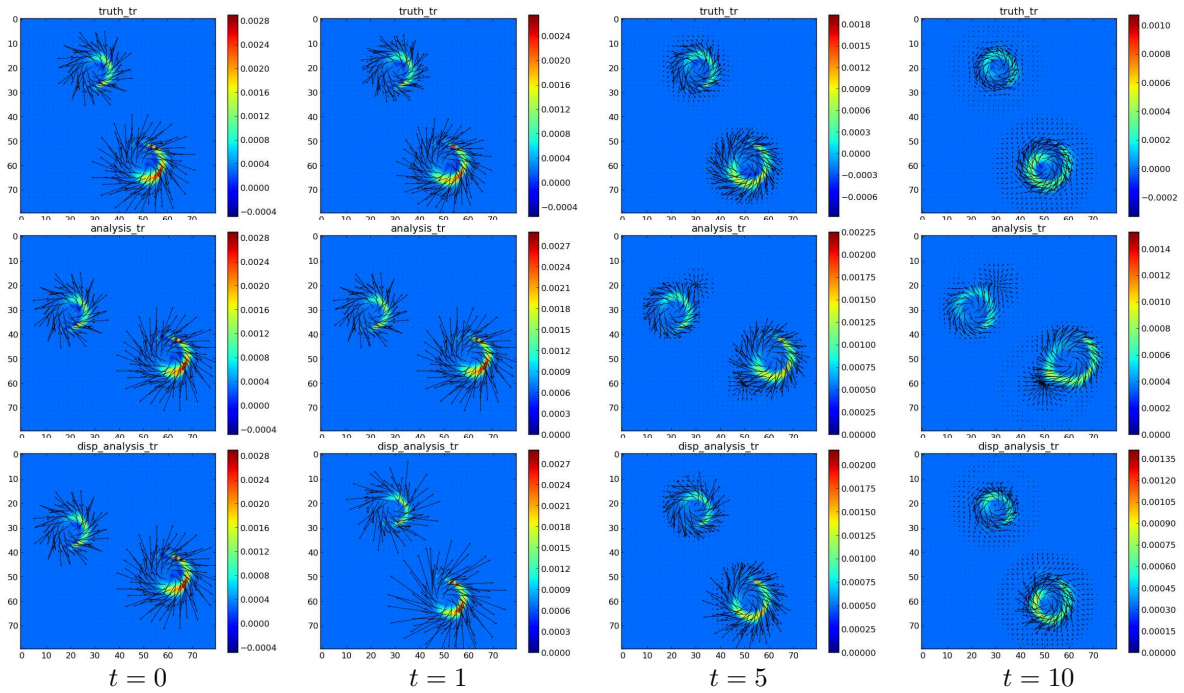

Fig. 4. State evolution of a passive tracer T along with the velocity vectors (u, v) of the shallow water model on 80x80 domain. Top row: measurements. Middle row: optimal interpolation assimilation. Bottom row: optimal interpolation with state alignment. The state alignment allows a better estimation of the velocity variables (u, v).

[3] I. M. Belkin and J. E. O'Reilly, "An algorithm for oceanic front detection in chlorophyll and sst satellite imagery," *J. of Marine Systems*, vol. 78, no. 3, pp. 319 – 326, 2009, special Issue on Observational Studies of Oceanic Fronts.

[4] J.-F. Cayula and P. Cornillon, "Edge detection algorithm for sst images," *J. of Atmospheric and Oceanic Technology*, vol. 9, no. 1, pp. 67–80, 1992.

[5] ——, "Multi-image edge detection for sst images," *J. of Atmospheric and Oceanic Technology*, vol. 12, no. 4, pp. 821–829, 1995.

[6] T. Corpetti, E. Mémin, and P. Pérez, "Dense estimation of fluid flows," *IEEE Trans. on Pattern Analysis and Machine Intelligence*, vol. 24, no. 3, pp. 365–380, 2002.

[7] L. Gaultier, J. Verron, J.-M. Brankart, O. Titaud, and P. Brasseur, "On the inversion of submesoscale tracer fields to estimate the surface ocean circulation," *to appear in J. of Marine Systems*, 2012.

[8] S. Gorthi, S. Béyou, T. Corpetti, and E. Mémin, "Multiscale weithed ensemble kalman filter for fluid flow estimation," in *Scale-Space and Variational Methods (SSVM'11)*, 2011.

[9] R. Guerin, G. Desroziers, and P. Arbogast, "4d-var analysis of potential vorticity pseudo-observations," *Quarterly J. of the Royal Meteorological Society*, vol. 132, no. 617, pp. 1283–1298, 2006.

[10] R. N. Hoffman, Z. Liu, J. F. Louis, and C. Grassotti, "Distortion representation of forecast errors," *Monthly Weather Review*, vol. 123, no. 9, pp. 2758–2770, 1995.

[11] J. Hopkins, P. Challenor, and A. G. P. Shaw, "A new statistical modeling approach to ocean front detection from sst satellite images," *J. of Atmospheric and Oceanic Technology*, vol. 27, no. 1, pp. 173–191, 2010.

[12] E. Huot, I. Herlin, N. Mercier, and E. Plotnikov, "Estimating apparent motion on satellite acquisitions with a physical dynamic model," in *Int. Conf. on Pattern Recognition (ICPR'10)*, 2010, pp. 41 –44.

[13] G. Lapeyre and P. Klein, "Dynamics of the upper oceanic layers in terms of surface quasigeostrophy theory." *J. of Physical Oceanography*, vol. 36, no. 2, pp. 165–176, 2006.

[14] W. G. Lawson and J. A. Hansen, "Alignment error models and ensemble-based data assimilation," *Monthly Weather Review*, vol. 133, no. 6, pp. 1687–1709, 2005.

[15] J. Marcello, F. Marques, and F. Eugenio, "Automatic tool for the precise detection of upwelling and filaments in remote sensing imagery," *IEEE Trans. on Geoscience and Remote Sensing*, vol. 43, no. 7, pp. 1605 – 1616, 2005.

[16] Y. Michel, "Data assimilation of tropopause height using dry intrusion observations," *Monthly Weather Review*, vol. 138, no. 1, pp. 101–122, 2010.

[17] P. Miller, "Multi-spectral front maps for automatic detection of ocean colour features from seawifs," *Int. J. of Remote Sensing*, vol. 25, no. 7-8, pp. 1437–1442, 2004.

[18] T. Nehrkorn, R. N. Hoffman, C. Grassotti, and J.-F. Louis, "Feature calibration and alignment to represent model forecast errors: Empirical regularization," *Quarterly J. of the Royal Meteorological Society*, vol. 129, no. 587, pp. 195–218, 2003.

[19] J. J. Oram, J. C. McWilliams, and K. D. Stolzenbach, "Gradient-based edge detection and feature classification of sea-surface images of the southern california bight," *Remote Sensing of Environment*, vol. 112, no. 5, pp. 2397 – 2415, 2008, earth Observations for Terrestrial Biodiversity and Ecosystems Special Issue.

[20] N. Papadakis and E. Mémin, "Variational assimilation of fluid motion from image sequence," *SIAM J. on Imaging Sciences*, vol. 1, pp. 343–363, 2008.

[21] S. Ravela, K. Emanuel, and D. McLaughlin, "Data assimilation by field alignment," *Physica D: Nonlinear Phenomena*, vol. 230, no. 1-2, pp. 127 – 145, 2007.

[22] D. Shepard, "A two-dimensional interpolation function for irregularly-spaced data," in *Proceedings of the 1968 23rd ACM national conference*, ser. ACM '68. New York, NY, USA: ACM, 1968, pp. 517–524.

[23] K. Simhadri, S. Iyengar, R. Holyer, M. Lybanon, and J. Zachary, "Wavelet-based feature extraction from oceanographic images," *IEEE Trans. on Geoscience and Remote Sensing*, vol. 36, no. 3, pp. 767 – 778, 1998.

[24] O. Titaud, A. Vidard, I. Souopgui, and F.-X. L. Dimet, "Assimilation of image sequences in numerical models," *Tellus A*, vol. 62, no. 1, 2010.

[25] X. Vigan, C. Provost, R. Bleck, and P. Courtier, "Sea surface velocities from sea surface temperature image sequences 1. method and validation using primitive equation model output," *J. Geophys. Res.*, vol. 105, no. C8, pp. 19 499–19 514, 2000.

[26] D. Wang, X. Liang, Y. Zhao, and B. Wang, "A comparison of two tropical cyclone bogussing schemes," *Weather and Forecasting*, vol. 23, no. 1, pp. 194–204, 2008.

[27] S. Y. Wu and A. K. Liu, "Towards an automated ocean feature detection, extraction and classification scheme for sar imagery," *Int. J. l of Remote Sensing*, vol. 24, no. 5, pp. 935–951, 2003.